Experimental Study of Compressible Turbulent Mixing Layers

Steven G. Goebel* and J. Craig Dutton†
University of Illinois at Urbana-Champaign, Urbana, Illinois 61801

Compressible, turbulent mixing layers have been investigated experimentally using pressure measurements, schlieren photographs, and velocity measurements with a two-component laser Doppler velocimeter system. Seven mixing-layer cases were examined, with relative Mach numbers ranging from 0.40 to 1.97, which spans the region of significant compressibility effects. Both the spatial development and similarity of the mixing layers were considered. The development of the mixing layers required a Reynolds number (based on the freestream velocity difference and local mixing-layer thickness) on the order of 1×10^5. In the fully developed regions of the mixing layers, it was found that transverse turbulence intensities and normalized kinematic Reynolds stresses decreased with increasing relative Mach number, whereas the streamwise turbulence intensities and kinematic Reynolds stress correlation coefficients remained relatively constant.

Nomenclature

a = speed of sound
b = mixing-layer thickness between transverse locations where $U = U_1 - 0.1\Delta U$ and $U = U_2 + 0.1\Delta U$
D = seed particle diameter
l = development length
l_m = mixing length, $= |\langle u'v' \rangle|^{1/2}/(\partial U/\partial y)$
M = Mach number
M_c = convective Mach number, $= \Delta U/(2\bar{a})$ (for streams with equal ratios of specific heats)
M_r = relative Mach number, $= \Delta U/\bar{a}$
P = static pressure
Re = unit Reynolds number, $= \bar{\rho}\Delta U/\bar{\mu}$
Re_b = Reynolds number based on b, $= \bar{\rho}\Delta U b/\bar{\mu}$
r = freestream velocity ratio, $= U_2/U_1$
s = freestream density ratio, $= \rho_2/\rho_1$
T = static temperature
T_t = total temperature
U = local mean streamwise velocity
u' = deviation of streamwise velocity from local mean
ΔU = freestream velocity difference, $= U_1 - U_2$
v' = deviation of transverse velocity from local mean
x = streamwise coordinate
y = transverse coordinate
y_0 = mixing-layer centerline (the midpoint between transverse locations where $U = U_1 - 0.1\Delta U$ and $U = U_2 + 0.1\Delta U$)
δ = boundary-layer thickness (transverse location where U is 99.5% of the freestream velocity)
θ = compressible boundary-layer momentum thickness
λ = velocity parameter, $= (1-r)/(1+r)$
λ_s = velocity-density parameter, $= [(1-r)(1+s^{1/2})]/[2(1+rs^{1/2})]$
μ = viscosity
ρ = density
ρ_p = density of seed particles
σ = standard deviation
$\langle\rangle$ = ensemble average
$\bar{}$ = average of freestream values

Subscripts
1 = primary stream
2 = secondary stream

Introduction

COMPRESSIBLE mixing layers are encountered within many practical devices such as supersonic ejectors for pumping and entrainment applications and in many scramjet engine designs for hypersonic vehicles. In the latter application, the performance of the engine is critcally dependent upon the entrainment, turbulent mixing, and combustion behavior of these compressible shear layers. In addition, compressible shear layers are a fundamental element of many other fluid flows.

The behavior of incompressible mixing layers has been studied extensively by several researchers (Batt,[1] Browand and Latigo,[2] Brown and Roshko,[3] Brown,[4] Liepmann and Laufer,[5] Miles and Shih,[6] Spencer,[7] and Wygnanski and Fiedler,[8] for example). While the incompressible works have provided a broad understanding of mixing layers, additional studies are required to explain the behavior of compressible mixing layers, that exhibit some differences in comparison to their incompressible counterparts. For example, it has been experimentally observed (Chinzei et al.,[9] Papamoschou and Roshko,[10] and others) that a supersonic mixing layer can grow much less quickly than an incompressible mixing layer at the same freestream velocity and density ratios.

A parameter, called the convective Mach number, has been proposed by Bogdanoff[11] to quantify the compressibility of a mixing layer and has been used to correlate the reduced growth rate of a compressible mixing layer, for example. A similar parameter has also been obtained by several analyses (Jackson and Grosch,[12] Ragab and Wu,[13] and Soetrisno et al.,[14] for example) which has been referred to as the relative Mach number M_r

$$M_r = \Delta U/\bar{a} \tag{1}$$

where ΔU is the freestream velocity difference and $\bar{a}$ is the average of the freestream speeds of sound. The major difference between the relative and convective Mach numbers is only in their derivations. The derivation of the convective Mach number is based upon a stagnation pressure balance between organized, large-scale structures; however, organized, large-scale structures have not been observed to be a dominant feature of fully developed, high-Reynolds number, compressible, turbulent mixing layers. In addition, the isentropic stagnation assumption used in the convective Mach number derivation may not be realistic, especially at larger convective Mach numbers. Papamoschou[15] has also observed that turbulent structures do not always convect at the velocity given by this analysis, particularly at higher convective Mach

Presented as Paper 90-0709 at the AIAA 28th Aerospace Sciences Meeting, Reno, NV, Jan. 8-11, 1990; received Feb. 23, 1990; revision received and accepted for publication April 24, 1990.

*Graduate Research Assistant, Department of Mechanical and Industrial Engineering. Student Member AIAA.
†Associate Professor, Department of Mechanical and Industrial Engineering. Member AIAA.

numbers. It therefore seems that the relative Mach number is a more appropriate parameter because it appears in compressible, free shear-layer analyses. It is also true that the relative and convective Mach numbers are proportional (by a factor of two) for mixing layers with streams having the same ratio of specific heats.

The relative Mach number has been shown to correlate normalized growth rates of compressible mixing layers (Chinzei et al.,[9] Papamoschou and Roshko,[10] and others) reasonably well when the growth rates of compressible mixing layers are normalized by the growth rates of an incompressible mixing layer at the same freestream velocity and density ratios. However, very few experimental investigations have considered the fluid dynamic details of compressible mixing layer behavior to explain this phenomenon. The present and related[16-18] studies and also the recent works of Samimy and Elliott[19] and Samimy et al.[20] are the only investigations that have obtained accurate and detailed measurements of the mean and turbulent velocity fields in developed, compressible mixing layers.

To better understand the fluid dynamic and combustion mechanisms that occur within a compressible, turbulent shear flow, an experimental facility has been developed at the University of Illinois for studying reacting and nonreacting compressible, turbulent mixing layers. Mixing layers at several operating conditions have been examined by using pressure measurements, schlieren photographs, and velocity measurements obtained with a two-component laser Doppler velocimeter (LDV) system. Experimental results for nonreacting, compressible, turbulent mixing layers at seven different operating conditions are reported herein.

Experimental Facilities

The wind tunnel used in this study was designed to produce a nominally two-dimensional mixing region over a length sufficient to allow full development of the mixing layer. A photograph of the test section with the LDV optics and traversing table in position is shown in Fig. 1. To obtain different operating conditions, the facilities have the capacity to independently heat the two air streams delivered to the stainless steel wind tunnel up to total temperatures of approximately 700 K by using a nonvitiated heat exchanger. A vitiated burner was also available that could provide combustible or noncombustible gas products at temperatures up to approximately 900 K; however, no reacting cases are presented here. Flow conditioning screens and honeycomb, as well as total pressure and total temperature probes for display and feedback to the system control valves, were located in each of the plenum chambers. The wind tunnel had replaceable nozzles with nominal Mach numbers of 2 and 2.4 for the primary stream and a Mach 1.4 secondary nozzle (which could also be run subsonically to increase the relative Mach number). The contours of these nozzle blocks were designed by the method of characteristics (Carroll et al.[21]) to produce uniform exit flow. The two streams were brought together to form the mixing layer at an angle of 2.5 deg across a thin splitter plate with a base height of approximately 0.5 mm. Each stream had an exit height of approximately 24 mm and a width of 96 mm. The divergence angle of the upper and lower walls of the test section was adjustable to allow control of the streamwise pressure gradient, although this adjustment was only effective when both streams were supersonic. Both sidewalls of the test section had quartz windows that could be mounted in two streamwise locations to give a total viewing length of approximately 500 mm. This optical access was necessary for both the LDV measurements and schlieren photographs. A pressure tap blank could also be mounted in place of one of the window frames, and a Pressure Systems Incorporated electronic pressure scanner was used to measure the sidewall static pressure distribution. The stagnation pressure in each plenum was controlled so that the static pressures of the two streams at the nozzle exits were matched. Also, the overall pressure level, the exit diffuser, and the upper and lower wall divergence angles were adjusted to produce the desired neutral pressure gradient for the compressible mixing layer.

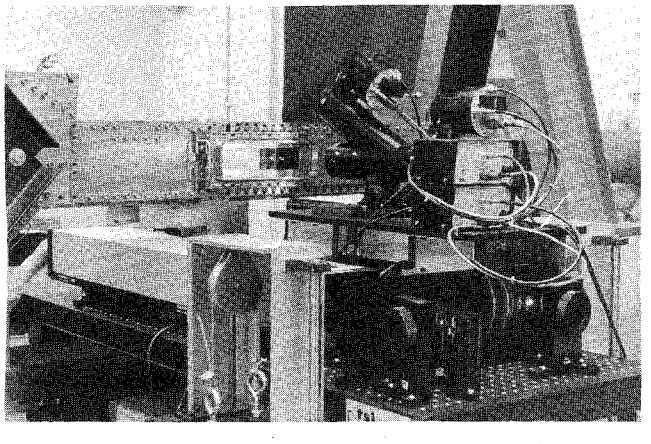

Fig. 1 Photograph of test section with LDV optics and traversing table.

A schlieren system has been used to visualize the mixing-layer flowfield. A Xenon spark light source (20 ns pulse duration) was used to "freeze" the flow. Lenses collimated the light, and three overlapping photographs were required to cover the length of each of the two streamwise window positions. Kodak T-Max 400 film was used in a 35 mm format camera with a macro lens and was processed using normal development.

A two-color, two-component, dual-beam Thermal Systems Incorporated LDV system has been employed to measure the mixing-layer velocity fields. The blue (488 nm wavelength) and green (514.5 nm wavelength) lines of a 4 W argon ion laser were used. The two components were oriented at ± 45 deg to the streamwise flow direction to minimize fringe biasing. The measurement volume was positioned by a custom-designed, computer-controlled, three-axis, traversing table. For the first three cases (cases 1, 1d, and 2), optical fibers transmitted the laser beams to a probe that resided, along with the receiving optics, on the traversing table. Unfortunately, the transmission capability of the optical fibers rapidly and permanently deteriorated with normal usage at the laser power levels necessary for these experiments. Therefore, the traversing table was extensively modified to increase its load-carrying capability, thus allowing the entire LDV optical system to be traversed by the table for the remaining four cases (cases 3, 3r, 4, and 5). Frequency counters processed the signals, and the two-channel coincidence window was adjusted to 1–2 μs. The data were transferred to a Macintosh II computer for storage, reduction, analysis, and plotting.

Two different arrangements of the LDV transmitting beams were used: one produced blue and green fringe spacings of 7.965 and 8.397 μm, respectively; and the second produced blue and green fringe spacings of 13.63 and 14.39 μm, respectively. The first arrangement was used for cases 1, 1d, 2, and 3; the larger fringe spacing was used for cases 3r, 4, and 5. Frequency shifting of 40 MHz was used for most of the cases (cases 3 through 5), and for these cases, the frequency counters were set to require eight fringe crossings in the single measurement per burst mode. For the other cases (cases 1, 1d, and 2), no frequency shifting was used, and four fringe crossings were required. For all cases, the collection optics were placed approximately 10 deg off the forward scatter axis. The effective measurement volume diameter and length were approximately 0.17 and 1.4 mm, respectively.

The two streams were seeded with titanium dioxide (TiO_2) particles from fluidized bed seeders, and the level of seeding of each stream was adjusted to produce comparable data rates in both freestreams. The average diameter of these particles was estimated to be 0.3 μm from the results of Bloomberg et al.[22]

by comparing their response to an oblique shock wave with the response of particles of known diameter and density (0.497 μm diam polystyrene latex [PSL] spheres). The effects of particle dynamics were further investigated by comparing velocity measurements for case 3 ($r = 0.18$, $s = 0.57$, and $M_r = 1.37$) obtained with 0.3 μm diam TiO_2 particles with those obtained with 0.497 μm diam PSL particles. Because of their much greater density, the TiO_2 particles have a response that is approximately 1.7 times slower than the PSL particles (the response time is approximately proportional to $\rho_p D^2$ but also depends on the Knudsen and Mach numbers), which is also supported by the work of Bloomberg et al.[22] It is to be noted that the TiO_2 seed particles were generally used for the results reported here due to their ability to withstand the high temperatures of the heated conditions. By comparing the measured profiles of mean and turbulent velocities obtained using these two types of particles with different response times, it was found that particle dynamics were not a problem in these measurements.[17,18]

For each case, transverse velocity profiles at several streamwise locations were obtained. Also, a one-component LDV arrangement was used to measure the streamwise velocity profiles of the splitter plate boundary layers at a streamwise location 2 mm upstream of the splitter plate tip. At each measurement location, at least 2000 velocity samples were taken. The data were not modified by any velocity debiasing scheme; however, a correction was made for fringe bias according to the analysis of Buchhave.[23] For more details on the experimental facilities, LDV system, and measurement procedures, see Goebel.[18]

Experimental Results

Seven mixing layer cases have been examined in this study. For each case, static pressures were measured, schlieren photographs were taken, and flowfield velocity measurements were obtained using an LDV system. These data have been used to obtain growth rates and to examine the development of the mean and turbulent velocity fields of compressible, turbulent mixing layers.

Operating Conditions

The operating conditions for the seven cases that have been examined are listed in Table 1. As is clear from this table, a wide variety of conditions has been studied with freestream velocity ratios ranging from 0.16 to 0.79, freestream density ratios ranging from 0.57 to 1.55, and relative Mach numbers ranging from 0.40 to 1.97. This range of relative Mach numbers spans the region of significant compressibility effects since at higher relative Mach numbers (i.e., above $M_r = 2.0$), Papamoschou and Roshko[10] found no further decreases in normalized growth rates.

Several of the cases were chosen to illustrate the isolated effects of mixing-layer parameters. Cases 1 and 1d illustrate the effects of freestream disturbances. For case 1d, the disturbed case, air was injected spanwise into the secondary plenum that increased the level of secondary freestream turbulence intensity, $\sigma_u/\Delta U$, to 0.13 in comparison to the undisturbed value of 0.05 for case 1. Cases 3 and 3r were performed to evaluate the isolated effects of velocity ratio on a compressible mixing layer, since the other parameters of freestream density ratio and relative Mach number were nearly the same for these two cases. Cases 3 and 4 demonstrate the isolated effects of relative Mach number as the other two parameters of freestream velocity and density ratio are nearly equal. Also, the cases are numbered in the order of increasing relative Mach number, i.e., in order of increasing compressibility effect.

The freestream velocities and pressures given in Table 1 are an average of the measured values from the region used to determine the mixing-layer growth rate, which is also given in Table 1. In terms of the average pressure, the maximum streamwise deviations in pressure were less than 6% for all of the cases with case 3r having the largest deviation. It should be mentioned that for case 3r, the static pressures of the two streams at the splitter plate tip could not be exactly matched to produce the desired freestream conditions. Therefore, a stronger compression wave was produced at the splitter plate tip, and this wave was reflected from the upper wall and back into the mixing-layer region. The maximum streamwise devia-

Table 1 Operating conditions, development lengths, and similarity values

Quantity	Case 1	Case 1d	Case 2	Case 3	Case 3r	Case 4	Case 5
$r = U_2/U_1$	0.78	0.79	0.57	0.18	0.25	0.16	0.16
$\lambda = (1-r)/(1+r)$	0.12	0.12	0.27	0.69	0.60	0.72	0.72
$s = \rho_2/\rho_1$	0.76	0.76	1.55	0.57	0.58	0.60	1.14
$\lambda_s = \frac{(1-r)(1+s^{1/2})}{2(1+rs^{1/2})}$	0.12	0.12	0.28	0.62	0.55	0.65	0.73
$M_r = \Delta U/\bar{a}$	0.40	0.40	0.91	1.37	1.44	1.73	1.97
M_c	0.20	0.20	0.46	0.69	0.72	0.86	0.99
M_1, M_2	2.01, 1,38	2.02, 1.39	1.91, 1.36	1.96, 0.27	2.22, 0.43	2.35, 0.30	2.27, 0.38
T_{t1}, T_{t2}, K	295, 295	275, 275	578, 295	285, 285	315, 285	360, 290	675, 300
U_1, U_2, m/s	515, 404	498, 392	700, 399	499, 92	561, 142	616, 100	830, 131
P, kPa	46	55	49	53	53	36	32
$Re = \bar{\rho}\Delta U/\bar{\mu}$ (10^6/m)	7.7	7.7	12	26	27	21	13
δ_1, δ_2, mm	2.5, 2.6	2.4, 2.4	2.9, 2.5	3.1, 3.0	1.6, 4.3	2.2, 1.7	1.7, 1.3
θ_1, θ_2, mm	0.20, 0.20	0.19, 0.20	0.29, 0.21	0.22, 0.36	0.12, 0.37	0.20, 0.17	0.10, 0.14
l_U, mm	300	125	100	25	50	10	10
$l_{\sigma u}$, mm	300	225	200	75	125	100	75
$l_{\sigma v}$, mm	300	475[a]	250	150	175[a]	125	100
$l_{\langle u'v'\rangle}$, mm	350	475[a]	250	150	175[a]	125	100
$Re_b = \bar{\rho}\Delta U b/\bar{\mu}(10^5)$, devel.	0.7	1.0[a]	1.3	2.5	3.4[a]	0.6	0.8
Growth region, mm	300-450	125-475	100-450	25-200	50-150	10-175	10-150
db/dx	0.020	0.026	0.038	0.059	0.058	0.050	0.049
Sim. locations, mm	350-450	325-375	300-400	150-200	125-175	100-150	75-125
$\sigma_u/\Delta U$, peak	0.22	0.21	0.17	0.18	0.16	0.18	0.18
$\sigma_v/\Delta U$, peak	0.15	0.15	0.099	0.078	0.086	0.065	0.053
σ_u/σ_v, peak	1.53	1.41	1.71	2.33	1.84	2.74	3.53
$-\langle u'v'\rangle/(\Delta U)^2$, peak	0.017	0.016	0.0086	0.0069	0.0073	0.0066	0.0058
$-\langle u'v'\rangle/(\sigma_u\sigma_v)$, mean	0.48	0.49	0.54	0.52	0.51	0.52	0.54
l_m/b, mean	0.15	0.15	0.11	0.090	0.092	0.088	0.086

[a]The mixing layer may not have been developed in terms of this quantity.

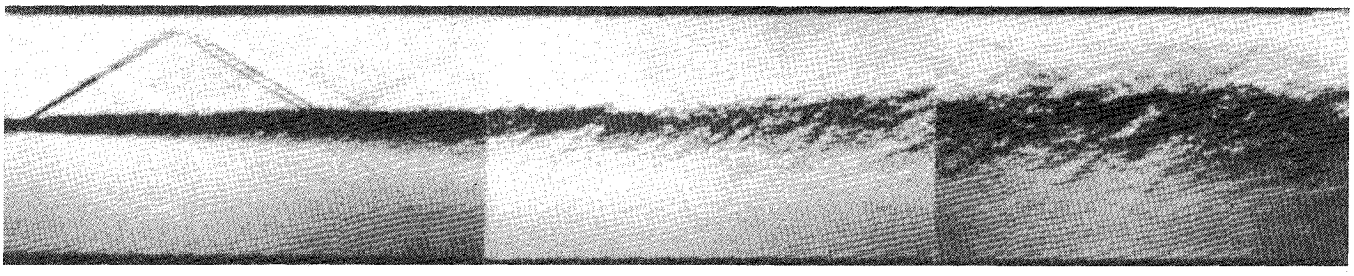

Fig. 2 Schlieren photographs of case 3.

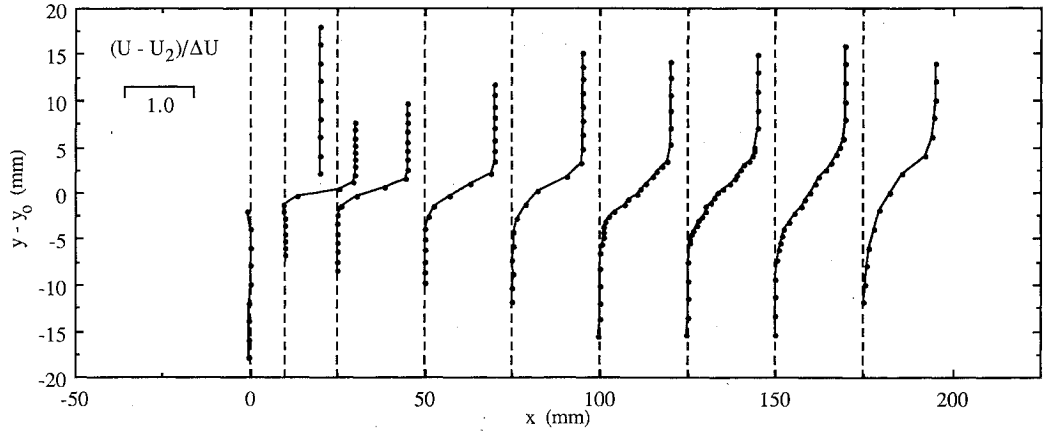

Fig. 3 Development of normalized mean streamwise velocity, $(U - U_2)/\Delta U$, for case 4.

tions in freestream velocity (expressed in terms of the velocity parameter λ) were largest for cases 1d and 2 with values of 17 and 13%, respectively, whereas for all of the other cases the deviations from the mean were less than 8%. Also note that the unit Reynolds numbers, $Re = \bar{\rho}\Delta U/\bar{\mu}$, are quite high in these experiments, ranging from 7.7 to 27 $\times 10^6$ (m^{-1}).

The splitter plate boundary-layer velocity profiles were also measured using a one-component LDV setup. From the level of measured turbulence intensities, the boundary layers were found to be turbulent for all of the cases, which was expected for these operating conditions. To estimate the boundary-layer thicknesses, the compressible, turbulent, boundary-layer velocity profile equation of Sun and Childs[24] was least-squares fit to the measured boundary-layer velocity profiles. The curve fit profiles were then used to determine the boundary-layer thicknesses and integrated to yield the compressible momentum thicknesses, both of which are given in Table 1.

Schlieren Photographs

Many flow features can be qualitatively seen in the 20 ns spark schlieren photographs of case 3 shown in Fig. 2. The flow is from left to right with the primary stream on top, and three photographs are required to cover the window that is in the upstream position. The splitter plate can be seen as it extends 8 mm into the field of view from the left, and the total length of the window is approximately 267 mm. Although compression and expansion waves originating from the splitter plate tip are evident in the photographs, they are not strong, as indicated by the pressure and freestream velocity measurements. More importantly, the mixing-layer behavior can be observed. The mixing layer appears to deflect slightly where it interacts with compression or expansion waves. Also, in these photographs, there do not appear to be any large-scale, two-dimensional, organized structures like those observed by Brown and Roshko[3] in low Reynolds number, incompressible mixing layers. In fact, only for cases 1 and 1d, which are at the lowest unit Reynolds number of those listed in Table 1, were any structures of this nature observed, and even then, these structures did not appear to dominate the mixing-layer character. The mixing layers under the conditions examined in this study appear to be characterized by much smaller turbulent structures. However, it should be mentioned that the schlieren technique provides an "integrated" visualization of the mixing layer over the width of the test section. Although many features can be qualitatively seen in the schlieren photographs, the mixing-layer thickness is difficult to pinpoint visually; therefore, the overall mixing-layer growth rate cannot be accurately determined from these photographs. Also, these photographs provide little quantitative information on the spatial development and similarity of the mixing layers.

Mixing-Layer Development

The flowfields evolve from two separate streams with boundary layers into fully developed mixing layers. Spatial development of transverse profiles of the mean streamwise velocity and transverse turbulence intensity for case 4 ($r = 0.16$, $s = 0.60$, and $M_r = 1.73$) are shown in Figs. 3 and 4, respectively. A mean velocity deficit initially exists that is due to the boundary layers shed from the splitter plate. However, because of the large velocity parameter λ of case 4, the velocity deficit is rapidly consumed as it has essentially been eliminated by the first measurement location, which was only 10 mm downstream of the splitter plate tip. Eventually, after the velocity deficit has been eliminated, the flowfield becomes fully developed. For a mixing layer to be considered fully developed, it is required that both the mean and turbulent velocity fields be self similar. Generally, the mean velocity field requires less streamwise distance to become self similar with increased development lengths being required for the streamwise turbulence intensity, transverse turbulence intensity, and Reynolds stress, respectively. Estimates of the lengths required for development of the streamwise mean velocity, streamwise turbulence intensity, transverse turbulence intensity, and kinematic Reynolds stress, l_U, $l_{\sigma u}$, $l_{\sigma v}$, $l_{\langle u'v'\rangle}$, respectively, are given in Table 1 for all of the cases. The development length for the mean velocity field was taken as the first streamwise location where a velocity deficit did not exist. The turbulence quantities were required to reach a constant peak value to be considered fully developed, as is demonstrated by the transverse turbulence intensity profiles in Fig. 4.

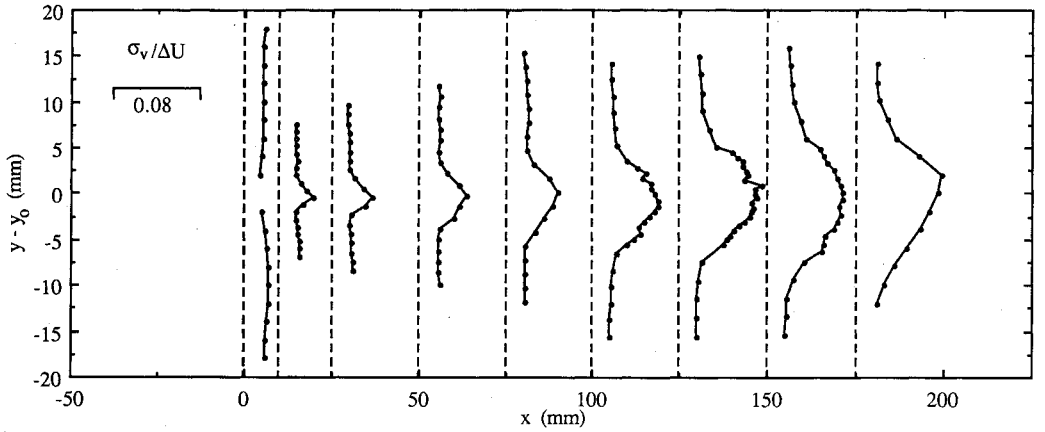

Fig. 4 Development of transverse turbulence intensity, $\sigma_v/\Delta U$, for case 4.

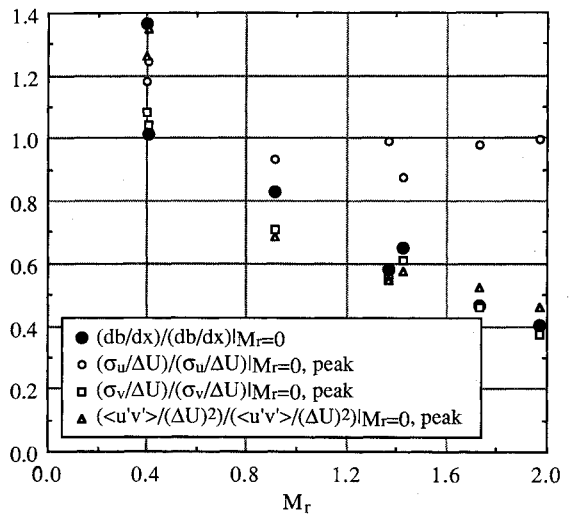

Fig. 5 Normalized growth rates and turbulence quantities vs relative Mach number.

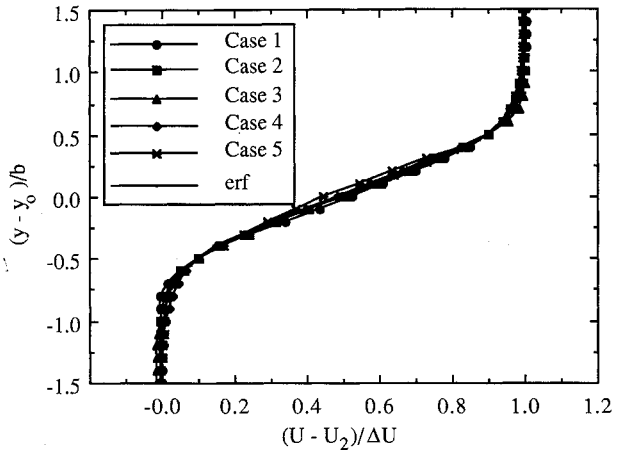

Fig. 6 Similarity profiles of normalized mean streamwise velocity.

Cases 1d and 3r may not have reached a fully developed state, particularly in terms of the transverse turbulence intensity and kinematic Reynolds stress. The full development of the turbulence field of case 1d was inhibited by the higher levels of secondary freestream turbulence because case 1, which was at the same operating conditions (except that the secondary stream was not disturbed), seems to have become more developed. Interestingly, the higher levels of secondary freestream turbulence of case 1d helped to eliminate the velocity deficit region due to the splitter plate boundary layers; therefore, the mean streamwise velocity appeared to become developed in less distance than was required for case 1. As was mentioned for the operating conditions of case 3r, the static pressures of the two streams at the splitter plate tip could not be exactly matched to produce the desired freestream conditions for this case; therefore, a stronger compression wave was produced at the splitter plate tip. This wave reflected between the upper wall and the mixing layer with reflections from the mixing layer occurring at approximately 75 and 150 mm downstream of the splitter plate tip. The interactions of this wave with the mixing layer may have disrupted the development of this case somewhat.

The requirements for full development of incompressible mixing layers have also been studied by Bradshaw.[25] For a single-stream shear layer, Bradshaw found that full development, in terms of Reynolds stress, required a Reynolds number based on streamwise distance $Re_x = \rho Ux/\mu$ of approximately 7×10^5 and that the initial thickness of the boundary layers, whether they were laminar or turbulent, had very little effect on the development length. An appropriate translation of this Reynolds number for application to heterogeneous and compressible two-stream mixing layers would be based upon the freestream velocity difference, the local mixing-layer thickness, and the average freestream properties. Based on Bradshaw's[25] result, the development criterion would then be a local Reynolds number with a value of approximately

$$Re_b = \bar{\rho}\Delta U b/\bar{\mu} = 1 \times 10^5 \qquad (2)$$

The local Reynolds number required for full development of the mean and turbulent velocity fields based on the mixing-layer thickness at the streamwise distance required for development of the kinematic Reynolds stress is listed in Table 1 for each of the current cases. This modified criterion also seems to approximately hold for the development of the compressible mixing layers presented here.

Mixing-Layer Similarity

Once a mixing layer has become fully developed, the velocity profiles can be expressed in self-similar form. The regions of the mixing layers where the mean streamwise velocity was considered to be self similar and that were used to determine the mixing-layer growth rates are listed in Table 1 as "Growth region." The mixing-layer growth rates are also listed in Table 1. To determine growth rates, a line was least-squares fit to the mixing-layer thickness data versus streamwise position. The mixing-layer thickness was taken to be the distance between transverse locations where the mean streamwise velocity was equal to $U_1 - 0.1\Delta U$ and $U_2 + 0.1\Delta U$. This mixing-layer thickness is very close to the vorticity thickness (approximately 1.02 times larger for an error function velocity profile) that has been used by Brown and Roshko[3] and others. Only thickness data from the region where the mean streamwise velocity

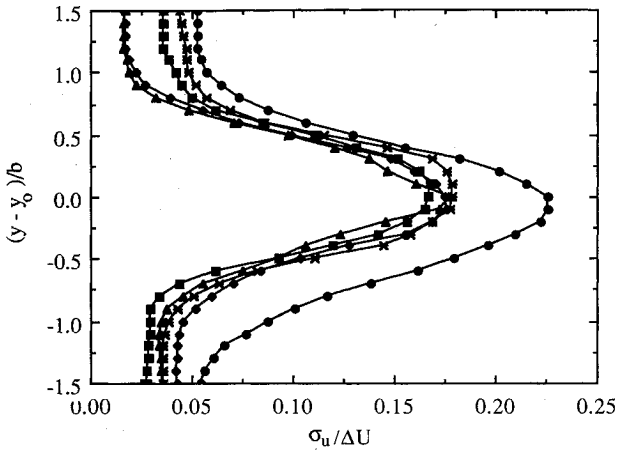

Fig. 7 Similarity profiles of streamwise turbulence intensity (symbols same as in Fig. 6).

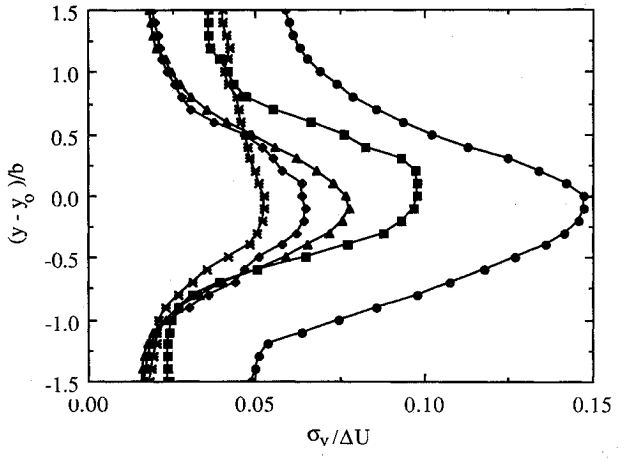

Fig. 8 Similarity profiles of transverse turbulence intensity (symbols same as in Fig. 6).

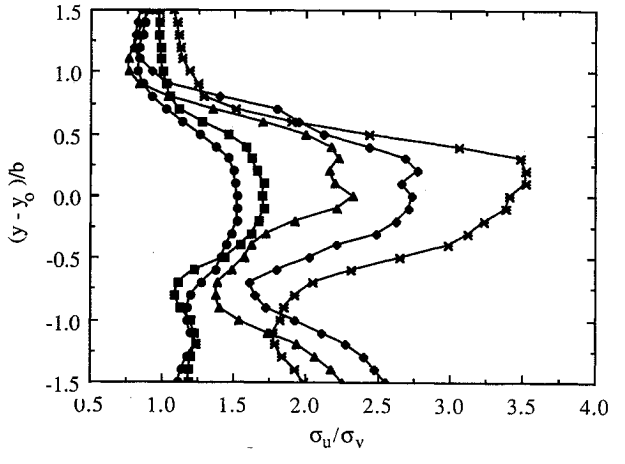

Fig. 9 Similarity profiles of anisotropy (symbols same as in Fig. 6).

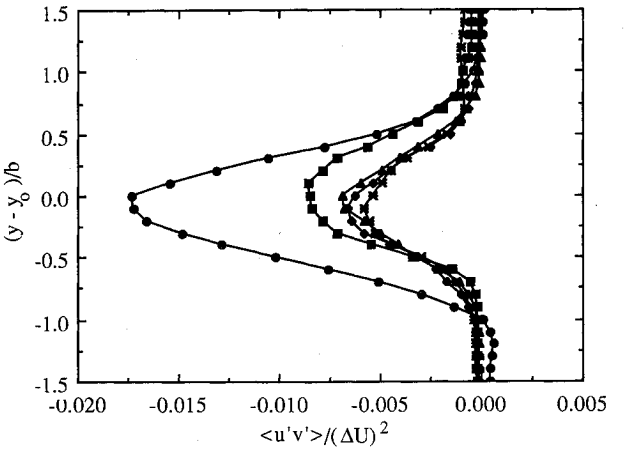

Fig. 10 Similarity profiles of normalized kinematic Reynolds stress (symbols same as in Fig. 6).

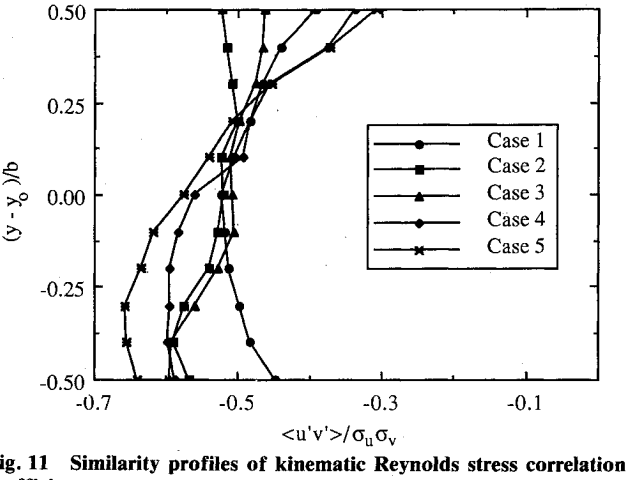

Fig. 11 Similarity profiles of kinematic Reynolds stress correlation coefficient.

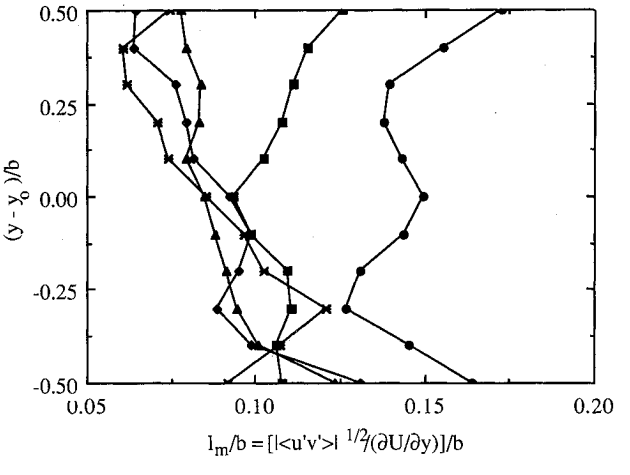

Fig. 12 Similarity profiles of normalized mixing length (symbols same as in Fig. 11).

was self similar were used to determine growth rates. The mixing-layer growth rates were normalized by the growth rate of the corresponding incompressible mixing layer at the same freestream velocity and density ratios, as given by Eq. (3), and these normalized growth rates are plotted in Fig. 5 with respect to relative Mach number:

$$db/dx|_{Mr=0} = 0.165\frac{(1-r)(1+s^{1/2})}{2(1+r\cdot s^{1/2})} \qquad (3)$$

The form of Eq. (3) was given by Papamoschou and Roshko,[10] and the constant was determined from the data of Spencer[7] and was scaled to the mixing-layer thickness definition used here. The results clearly show a growth rate reduction due to compressibility, and this reduction is consistent with that observed by others (Chinzei et al.[9] and Papamoschou and Roskho,[10] for example). Further insight into and explanation for this growth-rate reduction are provided by the velocity profiles presented below.

Fully developed profiles of the mean and turbulence quantities are shown in Figs. 6-12. For these plots, averaged profiles were used for each case. (Cases 1d and 3r were not included in these plots for clarity and since they are nearly identical to the

corresponding cases 1 and 3, respectively.) These profiles were obtained by averaging the normalized values from three profiles in the fully developed region at the same dimensionless transverse location $(y-y_0)/b$. Since data were not necessarily available at the same dimensionless transverse locations, linear interpolation was used to estimate values between data points. The streamwise locations of the profiles that were used to obtain the averaged profiles are listed in Table 1 as "Sim locations" for each case.

Fully developed profiles of the normalized mean streamwise velocity are shown in Fig. 6. Also shown is an error function profile, and each of the cases compares closely with the error function. An error function profile is used for comparison because it has been shown by Görtler (in Schlichting[26]) to be the first-order solution for the mean streamwise velocity profile of an incompressible, turbulent mixing layer. The error function also fits experimental data for incompressible mixing layers very well (Brown[4] or Spencer,[7] for example). It is interesting to note that even case 5, which has a significantly reduced growth rate in comparison to its incompressible counterpart and therefore was significantly affected by compressibility, has the same streamwise velocity profile shape as an incompressible mixing layer.

Streamwise turbulence intensity profiles have also been plotted in similarity form and are shown in Fig. 7. These profiles are comparable in shape and peak values for all of the cases except case 1. For case 1, the peak turbulence intensity is higher than for the other cases, which may be due to a lack of complete development of this near-wake case, and the higher levels of turbulence intensity that persist on the secondary side of the mixing layer that are a remnant of the velocity deficit region. The profiles of transverse turbulence intensities shown in Fig. 8 are quite different from the streamwise turbulence intensity profiles in that the peak values show a definite decrease with increasing relative Mach number. Again, effects similar to those mentioned for the streamwise turbulence intensity profile are present in the transverse turbulence intensity profile of case 1.

From the two components of turbulence intensity, the anisotropy, σ_u/σ_v, of the turbulence can be determined, and similarity profiles of anisotropy are plotted in Fig. 9. Since the transverse turbulence intensity decreases and the streamwise turbulence intensity remains nearly constant with increasing relative Mach number, the anisotropy, as can be seen in Fig. 9, increases substantially with increasing relative Mach number. Therefore, it would seem that numerical simulations that are based on isotropic turbulence models may perform poorly at higher relative Mach numbers.

Decreases similar to those observed in the transverse turbulence intensity are also observed in the normalized kinematic Reynolds stress with increasing relative Mach number, as shown in Fig. 10. Since Reynolds stress represents a transverse transport of streamwise momentum, these reduced values clearly would have a significant effect on mixing-layer growth rates.

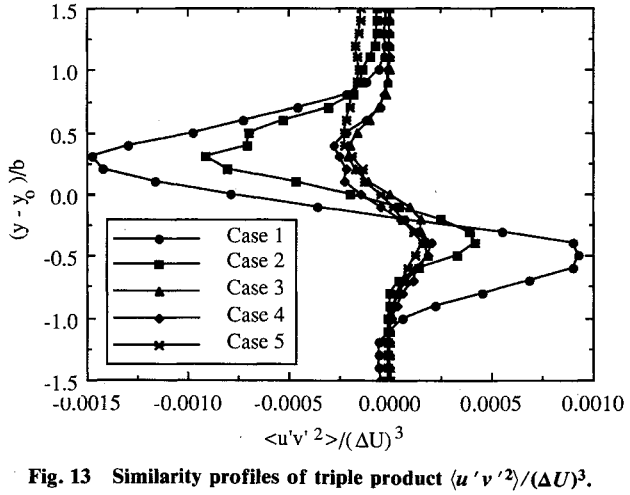

Fig. 13 Similarity profiles of triple product $\langle u'v'^2\rangle/(\Delta U)^3$.

Another useful observation is that the kinematic Reynolds stress correlation coefficient $\langle u'v'\rangle/\sigma_u\sigma_v$ is nearly constant across the central mixing-layer region, and its value is nearly the same for all of the cases, as is shown by Fig. 11. The average value of the kinematic Reynolds stress correlation coefficient between the dimensionless transverse coordinates of ± 0.5 is given in Table 1. An additional measure of turbulent structure is the mixing length defined as $l_m = |\langle u'v'\rangle|^{1/2}/(\partial U/\partial y)$ and shown in normalized form (divided by the local mixing-layer thickness) in Fig. 12. An average value of this quantity through the central region of the mixing layer is also given in Table 1 for each case. The normalized mixing length also decreases with increasing relative Mach number.

Higher order velocity products, such as the triple product $\langle u'v'^2\rangle/(\Delta U)^3$ shown in Fig. 13, can also be calculated from the ensembles of measured instantaneous velocities. Triple products represent the turbulent transport of turbulent kinetic energy. In Fig. 13, the peak values of this product, which contains a transverse velocity fluctuation contribution, are seen to decrease with increasing relative Mach number. The level of other triple products (not presented here) that contain a transverse velocity fluctuation contribution also decrease with increasing relative Mach number; however, the correlation coefficients of triple products did not seem to be substantially affected by changes in relative Mach number.

Effect of Compressibility

The peak values of the normalized Reynolds stress, as well as the peak values of the turbulence intensities and anisotropy in the similarity region, are listed in Table 1 for all of the cases. The turbulence quantities have been normalized by the freestream velocity difference because fully developed, peak turbulence intensities so normalized have been observed to be nearly constant for incompressible mixing layers over a wide range of velocity and density ratios. From the data of Batt,[1] Browand and Latigo,[2] Spencer,[7] and Wygnanski and Fiedler,[8] the peak values of the normalized turbulence quantities $\sigma_u/\Delta U$, $\sigma_v/\Delta U$, and $-\langle u'v'\rangle/(\Delta U)^2$ in the fully developed region of incompressible mixing layers have been measured to be in the ranges of 0.17–0.18, 0.13–0.14, and 0.01–0.013, respectively. Therefore, variations in compressible mixing-layer data from incompressible values should reflect the effects of compressibility. The peak values of $\sigma_u/\Delta U$, $\sigma_v/\Delta U$, and $-\langle u'v'\rangle/(\Delta U)^2$ for the current cases have been normalized by the respective values for incompressible mixing layers and are plotted in Fig. 5. The incompressible peak values of $\sigma_u/\Delta U$, $\sigma_v/\Delta U$, and $-\langle u'v'\rangle/(\Delta U)^2$ used for normalization were 0.18, 0.14, and 0.013, respectively. As can be seen in Fig. 55, both the normalized transverse turbulence intensity and the normalized kinematic Reynolds stress decrease with relative Mach number like the normalized growth rate. However, the normalized streamwise turbulence intensity remains nearly constant with relative Mach number. From order-of-magnitude estimates using boundary-layer approximations to the governing equations, it can be shown that for a compressible mixing layer the normalized kinematic Reynolds stress should scale with the normalized growth rate.[3] Numerical simulations of compressible mixing layers by Burr and Dutton[27] are also in agreement with the trend of decreasing transverse turbulence intensity while the streamwise turbulence intensity remains constant with increasing relative Mach number. Therefore, it is proposed that the normalized growth rate of a compressible shear layer decreases like the normalized kinematic Reynolds stress and that the transverse turbulence intensity similarly decreases while the streamwise turbulence intensity remains nearly constant with increasing relative Mach number. From the simulations of Burr and Dutton,[27] it is believed that the reduction of transverse turbulence intensity is due to the suppression of the pressure-transverse velocity correlation that

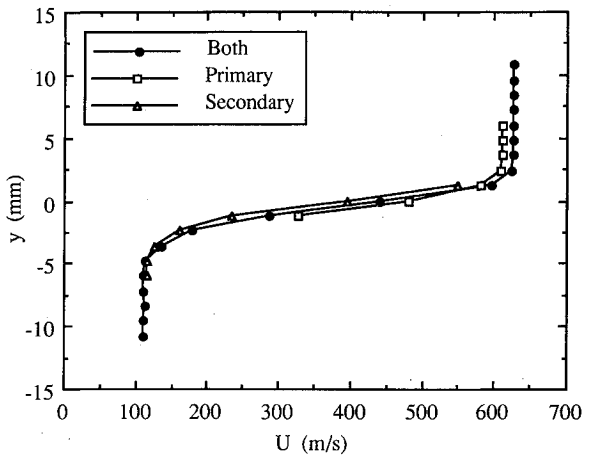

Fig. 14 Single-stream seeded mean streamwise velocity profiles for case 4 at $x = 50$ mm.

redistributes turbulent kinetic energy from the streamwise to the transverse direction. This reduction in pressure-transverse velocity correlation may be caused by the decrease in the domain within which pressure waves can propagate due to the increased relative Mach number of the flow.

Referring to the data in Fig. 5, some discrepancies from the trends mentioned above occur for the lowest relative Mach number cases (cases 1 and 1d). This may be due to a few factors particular to these cases: first, these cases may not be completely developed, and second, the freestream velocity difference was much smaller for these cases, making the results subject to a larger percentage error in terms of this velocity difference. Finally, these cases were close to a wake case with velocity ratios of nearly 0.8. In addition, the data for case 3r do not follow the stated trends as closely as the remaining cases, which may be due to the greater nonuniformity of the freestream velocity and streamwise pressure gradients caused by the stronger waves for this case. As stated earlier, these waves originated at the splitter plate tip and were due to a slight mismatch in nozzle exit static pressures.

Comparisons between cases that isolated the effects of a single parameter indicate that the relative Mach number is an appropriate measure of compressibility effects. Cases 3 and 3r illustrate the effects of changing the freestream velocity ratio while the freestream density ratio and relative Mach number are held nearly constant. Despite the difficulties with case 3r that were discussed above, the agreement between normalized values of cases 3 and 3r shown in Fig. 5 indicates that the effects of compressibility are primarily determined by the relative Mach number and are not a function of the velocity parameter. Cases 3 and 4 illustrate the isolated effect of relative Mach number since the freestream velocity and density ratios are nearly identical for these two cases. Comparisons between the results shown in Fig. 5 for cases 3 and 4 clearly demonstrate the trends of decreasing normalized growth rate, transverse turbulence intensity, and kinematic Reynolds stress with increasing relative Mach number. Also, the streamwise turbulence intensity was very similar for these two cases.

Single-Stream Seeding

To examine the behavior of fluid entrained into the mixing layer and to determine the effects of particle concentration biasing, i.e., whether seeding the two freestreams at different concentrations affects the measured velocity statistics, single-stream seeding experiments were conducted. Figure 14 shows the mean streamwise velocity profiles for case 4 at 50 mm downstream of the splitter plate tip when only the primary or secondary stream was seeded, as well as when both streams were seeded at a level to produce comparable freestream data rates. When only one stream was seeded, the profiles do not extend across the mixing layer because data rates beyond the locations for which measurements are shown indicated that a statistically significant portion of the samples could have been obtained from residual particles from the unseeded stream. The reduced data rates on the unseeded side of the mixing layer were a result of lower concentrations of the seeded fluid in that region. Although this penetration of seeded fluid gives an indication of the mixed region, the measurement grid used at this location was too coarse to determine accurately the mixed region thickness on this basis. In terms of particle concentration biasing, as Fig. 14 illustrates, the mean velocity profile is virtually the same regardless of which stream, or both, is seeded. This indicates that fluid within the mixing layer has the same mean streamwise velocity regardless of from which freestream the fluid originated, and it also demonstrates that particle concentration biasing does not affect the measured mean streamwise velocity for this flowfield. Although not shown here, similar comments also apply to the turbulence intensities and kinematic Reynolds stress.

Conclusions

The above discussion is a condensed summary of an experimental study of compressible, turbulent mixing layers. Some of the more important findings are listed below.

1) From the schlieren photographs, organized, large-scale structures were not observed under the high Reynolds number, compressible conditions studied here.

2) The length required for the mixing layers to develop generally increased in the order of mean streamwise velocity, streamwise turbulence intensity, and transverse turbulence intensity, followed by kinematic Reynolds stress.

3) Full development of the mixing layers (in terms of the development of kinematic Reynolds stress) required a local Reynolds number $Re_b = \bar{\rho}\Delta U b/\bar{\mu}$ of approximately 1×10^5.

4) Higher levels of freestream turbulence and shock waves inhibited and disrupted the mixing-layer development process.

5) Fully developed streamwise mean velocity profiles were well approximated by an error function profile even for the more compressible cases.

6) Normalized mixing-layer growth rates decreased with increasing relative Mach number, and the relative Mach number seems to be an adequate parameter for correlating the effects of compressibility.

7) Transverse turbulence intensities and normalized kinematic Reynolds stresses both decreased like normalized growth rates with increasing relative Mach number. Mixing lengths and other turbulence quantities with a transverse fluctuation velocity component also decreased with increasing relative Mach number.

8) Streamwise turbulence intensities remained fairly constant with relative Mach number. Therefore, since the transverse turbulence intensity decreased with increasing relative Mach number, the anisotropy σ_u/σ_v of the turbulence increased with increasing relative Mach number.

9) Kinematic Reynolds stress correlation coefficients were also found to remain approximately constant with relative Mach number, and the profiles were fairly flat across the central region of the mixing layers. Also, other correlation coefficients did not seem to be affected by changes in relative Mach number.

10) From the single-stream seeding experiments, it was found that fluid within the mixing layer had the same mean streamwise velocity regardless of from which freestream the fluid originated, and also it was shown that particle concentration biasing did not affect the velocity measurements.

Acknowledgments

This research was sponsored by the Office of Naval Research, R. S. Miller and G. D. Roy, contract monitors, and the Johns Hopkins University Applied Physics Laboratory, G. A. Sullins, contract monitor. The authors would like to thank the following colleagues for their assistance and support: Ron Adrian, Herman Krier, and John Renie; Robert Coverdill;

Ron Burr, Rich DeLoof, Bill Frantz, Nathan Messersmith, and Ralph Metcalf; and Kirk Kruenegel.

References

[1]Batt. R. G., "Turbulent Mixing of Passive and Chemically Reacting Species in a Low-Speed Shear Layer," *Journal of Fluid Mechanics,* Vol. 82, Aug. 1977, pp. 53–95.

[2]Browand, F. K., and Latigo, B. O., "Growth of the Two-Dimensional Mixing Layer from a Turbulent and Nonturbulent Boundary Layer," *Physics of Fluids,* Vol. 22, June 1979, pp. 1011–1019.

[3]Brown, G. L., and Roshko, A., "On Density Effects and Large Structure in Turbulent Mixing Layers," *Journal of Fluid Mechanics,* Vol. 64, July 1974, pp. 775–816.

[4]Brown, J. L., "Heterogeneous Turbulent Mixing Layer Investigations Utilizing a 2-D 2-Color Laser Doppler Anemometer and a Concentration Probe," Ph.D. Thesis, Univ. of Missouri-Columbia, Columbia, MO, 1978.

[5]Liepmann, H. W., and Laufer, J., "Investigations of Free Turbulent Mixing," NACA TN-1259, 1947.

[6]Miles, J. B., and Shih, J. S., "Similarity Parameter for Two-Stream Turbulent Jet-Mixing Region," *AIAA Journal,* Vol. 6, July 1968, pp. 1429–1430.

[7]Spencer, B. W., "Statistical Investigation of Turbulent Velocity and Pressure Fields in a Two-Stream Mixing Layer," Ph.D. Thesis, Dept. of Nuclear Engineering, Univ. of Illinois, Urbana, IL, 1970.

[8]Wygnanski, I., and Fiedler, H. E., "The Two-Dimensional Mixing Region," *Journal of Fluid Mechanics,* Vol. 41, April 1970, pp. 327–361.

[9]Chinzei, N., Masuya, G., Komuro, T., Murakami, A., and Kudou, K., "Spreading of Two-Stream Supersonic Turbulent Mixing Layers," *Physics of Fluids,* Vol. 29, May 1986, pp. 1345–1347.

[10]Papamoschou, D., and Roshko, A., "The Compressible Turbulent Shear Layer: An Experimental Study," *Journal of Fluid Mechanics,* Vol. 197, Dec. 1988, pp. 453–477.

[11]Bogdanoff, D. W., "Compressibility Effects in Turbulent Shear Layers," *AIAA Journal,* Vol. 21, June 1983, pp. 926–927.

[12]Jackson, T. L., and Grosch, C. E., "Absolute/Convective Instabilities and the Convective Mach Number in a Compressible Mixing Layer," ICASE Rept. 89-38, June 1989.

[13]Ragab, S. A., and Wu, J. L., "Instabilities in the Free Shear Layer Formed by Two Supersonic Streams," AIAA Paper 88-0038, Jan. 1988.

[14]Soetrisno, M., Eberhardt, S., Riley, J. J., and McMurtry, P., "A Study of Inviscid, Supersonic Mixing Layers Using a Second-Order Total Variational Diminishing Scheme," *AIAA Journal,* Vol. 27, Dec. 1989, pp. 1770–1778.

[15]Papamoschou, D., "Structure of the Compressible Turbulent Shear Layer," AIAA Paper 89-0126, Jan. 1989.

[16]Goebel, S. G., Dutton, J. C., Krier, H., and Renie, J. P., "Mean and Turbulent Velocity Measurements of Supersonic Mixing Layers," *Eleventh Symposium on Turbulence,* Paper A34, University of Missouri-Rolla, Rolla, MO, Oct. 1988 (see also Goebel, S. G., Dutton, J. C., Krier, H., and Renie, J. P., "Mean and Turbulent Velocity Measurements of Supersonic Mixing Layers," *Experiments in Fluids,* Vol. 8, Feb. 1990, pp. 263–272).

[17]Goebel, S. G., and Dutton, J. C., "Velocity Measurements of Compressible, Turbulent Mixing Layers," AIAA Paper 90-0709, Jan. 1990.

[18]Goebel, S. G., "An Experimental Investigation of Compressible, Turbulent Mixing Layers," Ph.D. Thesis, Dept. of Mechanical and Industrial Engineering, Univ. of Illinois, Urbana, IL, 1990.

[19]Samimy, M., and Elliott, G. S., "Effects of Compressibility on the Structure of Free Shear Layers," AIAA Paper 88-3054, July 1988.

[20]Samimy, M., Erwin, D. E., and Elliott, G. S., "Compressibility and Shock Wave Interaction Effects on Free Shear Layers," AIAA Paper 89-2460, July 1989.

[21]Carroll, B. F., Dutton, J. C., and Addy, A. L., "NOZCS2: A Computer Program for the Design of Continuous Slope Supersonic Nozzles," Univ. of Illinois, Urbana, IL, Eng 86-4007, Aug. 1986.

[22]Bloomberg, J. E., Dutton, J. C., and Addy, A. L., "An Investigation of Particle Dynamics Effects Related to LDV Measurements in Compressible Flows," Dept. of Mechanican and Industrial Engineering, Univ. of Illinois, Urbana, IL, Rept. No. UILU ENG 89-4009, Sept. 1989.

[23]Buchhave, P., "Biasing Errors in Individual Particle Measurements with the LDA-Counter Signal Processor," *The Accuracy of Flow Measurements by Laser Doppler Methods, Proceedings of the LDV- Symposium, Copenhagen,* Hemisphere, New York, 1975, pp. 258–278.

[24]Sun, C. C., and Childs, M. E., "A Modified Wall Wake Velocity Profile for Turbulent Compressible Boundary Layers," *Journal of Aircraft,* Vol. 10, June 1973, pp. 381–383.

[25]Bradshaw, P., "The Effects of Initial Conditions on the Development of a Free Shear Layer," *Journal of Fluid Mechanics,* Vol. 26, Oct. 1966, pp. 225–236.

[26]Schlichting, H., *Boundary-Layer Theory,* 7th ed., McGraw-Hill, New York, 1979, pp. 737–738.

[27]Burr, R. F., and Dutton, J. C., "Numerical Modeling of Compressible Reacting Turbulent Shear Layers," AIAA Paper 90-1463, June 1990.